Aerodynamic Properties of Spherical Balloon Wind Sensors

GEORGE H. FICHTL

Aerospace Environment Division, NASA-George C. Marshall Space Flight Center, Huntsville, Ala. 35812

AND R. E. DEMANDEL AND S. J. KRIVO

Lockheed Missiles & Space Company, Huntsville, Ala. 35812

(Manuscript received 26 July 1971, in revised form 24 November 1971)

ABSTRACT

A first-order theory of the fluctuating lift and drag coefficients associated with the aerodynamically induced motions of rising and falling spherical wind sensors is developed. The equations of motion of a sensor are perturbed about an equilibrium state in which the buoyancy force balances the mean vertical drag force. It is shown that, to within first order in perturbation quantities, the aerodynamic lift force is confined to the horizontal, and the fluctuating drag force associated with fluctuations in the drag coefficient acts along the vertical. The perturbation equations are transformed with Fourier-Stieltjes integrals and the resulting equations lead to relationships between the power spectra of the aerodynamically induced velocity components and the spectra of the fluctuating lift and drag coefficients.

Experimental evidence shows that the aerodynamically induced motions of the Jimsphere balloon occur predominantly in the horizontal plane. This implies that the root-mean-square (rms) horizontal lift coefficient is much larger than the rms vertical drag coefficient. The aerodynamically induced motion of the Jimsphere is found to be sinusoidal in nature. The dimensionless frequency (Strouhal number) and nondimensional variance of the induced zonal and meridional velocity components are given as functions of the Reynolds number. The experimental range of the Reynolds number is 1.4×10^5 to 6.6×10^5. The ratio between the rms lift coefficient and the mean, or zero-order, drag coefficient is found to be approximately 0.36.

The theory shows that the Fourier components of the first-order fluctuating horizontal lift coefficient vector lead those of the induced horizontal velocity vector, and that the fluctuating part of the drag coefficient lags the induced vertical velocity for rising balloons and leads the induced vertical velocity in the case of falling balloons. The phase angles of the induced lift and drag associated with the characteristic frequency of oscillation of the Jimsphere are given as functions of the Reynolds number.

The rms lift coefficient of smooth 2 m ROSE balloons operating at supercritical Reynolds numbers is found to be approximately twice the value obtained from wind tunnel data. This result suggests that caution should be exercised when wind tunnel data of constrained bodies are applied to free balloons.

1. Introduction

In deriving high-quality wind information from measurements of the motions of balloon wind sensors, three factors must be considered: 1) the response of the sensors to the environmental wind, 2) the accuracy of the tracking system, and 3) the aerodynamically induced motions of the sensor. This investigation is concerned with the third factor. Sensor motions, produced by aerodynamic lift forces normal to the velocity vector of the air relative to the balloon, result from the shedding of vorticity. These motions are controlled by the physical characteristics of the balloon (shape, weight, distribution of mass, etc.) and the dynamic and thermodynamic properties of the air. It is known that there are significant differences between the aerodynamic properties of smooth and roughened spherical balloons. The addition of roughness elements serves to control vortex shedding in supercritical Reynolds number (based on the balloon diameter and rise rate) flow, thereby decreasing the spectral bandwidth of aerodynamically induced motions.

Aerodynamically induced motions may introduce significant errors into the wind calculations. The spectral properties of balloon motions can be specified in terms of the spectra of the aerodynamic lift and drag force coefficients. Once these power spectra are known, it is possible, in principle, to develop filters which can remove the aerodynamically induced motions from balloon tracking data. Knowledge of the coefficients could also aid in the design of meteorological balloons.

The purpose of this investigation is twofold: 1) to develop a linear perturbation theory of balloon motion, whereby it is possible to calculate spectra of the aerodynamic coefficients from velocity spectra of self-induced balloon motions, and 2) to apply this theory to extend present knowledge of the aerodynamic properties of roughened and smooth spherical wind sensors.

Unauthenticated | Downloaded 09/20/24 07:16 PM UTC

2. Basic equations

The basic vector equation of the motion of a balloon or falling sphere wind sensor is given by

$$m\frac{d\mathbf{V}}{dt}=\tfrac{1}{2}\rho C_D A|\mathbf{V}_e-\mathbf{V}|(\mathbf{V}_e-\mathbf{V})+\tfrac{1}{2}\rho\mathbf{C}_L A|\mathbf{V}_e-\mathbf{V}|^2 +m_a\frac{d}{dt}(\mathbf{V}_e-\mathbf{V})-(m-m_0)g\mathbf{k}, \quad (1)$$

where m, m_a, A, $\mathbf{C}_L$ and C_D denote the mass, apparent mass, cross-sectional area, the lift coefficient vector, and drag coefficient of the sensor, respectively. The symbol m_0 is the mass of air displaced by the sensor, g the acceleration of gravity, ρ ambient density, and t time. The quantities $\mathbf{V}$ and $\mathbf{V}_e$ denote the velocity vectors of the sensor and the environment.

The first and second terms on the right-hand side of (1) represent the aerodynamic drag and lift forces. The drag force is parallel and opposite in direction to the relative wind vector $(\mathbf{V}_e-\mathbf{V})$. The aerodynamic lift force is normal to the relative wind vector. The third term represents the apparent mass effect (Reed, 1963), and the fourth term the buoyant force.

3. First-order perturbation equations

The environmental wind is assumed to be composed of a constant, basic state horizontal flow and a superimposed velocity perturbation, so that the zonal, meridional and vertical components are given by

$$\left.\begin{aligned} u_e(t)&=\bar{u}_e+u_e'(t)\\ v_e(t)&=\bar{v}_e+v_e'(t)\\ w_e(t)&=w_e'(t)\end{aligned}\right\}. \quad (2)$$

The overbars and primes denote the basic state and fluctuating parts of the wind. The velocity components of the sensor, $u(t)$, $v(t)$ and $w(t)$, are similarly represented except that, unlike the assumed environment, the sensor has a mean vertical velocity $\bar{w}$. One assumes that all perturbation quantities are infinitesimal or sufficiently small that second- and higher-order terms in perturbation quantities can be neglected with respect to first-order terms. Furthermore, it is assumed that the horizontal mean motion of the sensor is in equilibrium with the mean flow of the environment; thus, $\bar{u}=\bar{u}_e$ and $\bar{v}=\bar{v}_e$.

a. The lift forces

The aerodynamic lift forces act in a plane perpendicular to the relative wind vector and result from vortex shedding and wake instability. Variations in the magnitude and direction of these forces are responsible for the aerodynamically induced motions exhibited by wind sensors like the ROSE (Engler, 1965; Brockman, 1964) and the Jimsphere (Scoggins, 1967) balloons. The zonal, meridional and vertical components, C_{Lx}, C_{Ly}, C_{Lz}, of the lift coefficient vector can be functions of time and are treated as perturbation quantities. Since the lift vector acts in a plane perpendicular to the relative wind vector, the orientation of this plane is defined by the two vectors $\mathbf{i}\times(\mathbf{V}_e-\mathbf{V})$ and $\mathbf{j}\times(\mathbf{V}_e-\mathbf{V})$. It then follows that two unit vectors which define the orientation of the lift plane, to within first-order terms, are given by

$$\left.\begin{aligned}\mathbf{N}_1&=\frac{\bar{w}}{|\bar{w}|}\left[\mathbf{j}+\frac{(v_e'-v')}{\bar{w}}\mathbf{k}\right]\\ \mathbf{N}_2&=\frac{\bar{w}}{|\bar{w}|}\left[\mathbf{i}+\frac{(u_e'-u')}{\bar{w}}\mathbf{k}\right]\end{aligned}\right\}, \quad (3)$$

where $\mathbf{i}$, $\mathbf{j}$ and $\mathbf{k}$ are the standard unit vectors. These results show that the plane of the lift force is tilted only slightly from the horizontal. Utilization of the unit vectors given by (3) permits the lift coefficient to be expressed as

$$\mathbf{C}_L=C_2\mathbf{i}+C_1\mathbf{j}+\left[C_1\frac{(v_e'-v')}{\bar{w}}+C_2\frac{(u_e'-u')}{\bar{w}}\right]\mathbf{k}, \quad (4)$$

where C_2 and C_1 are the components of $\mathbf{C}_L$ directed along $\mathbf{N}_1$ and $\mathbf{N}_2$. Clearly, $C_2=C_{Lx}$ and $C_1=C_{Ly}$ to within first-order terms, and C_{Lz} is therefore a second-order perturbation quantity. In other words, the first-order aerodynamic lift force is confined to the horizontal plane.

Substitution of the perturbation expansions for $\mathbf{V}_e$ and $\mathbf{V}$ into the lift force term in (1) and utilization of the above result yield the first-order lift force

$$\mathbf{F}_L=\tfrac{1}{2}\rho A\bar{w}^2(C_{Lx}\mathbf{i}+C_{Ly}\mathbf{j}). \quad (5)$$

b. The drag force

The drag coefficient can be represented as a sum of a mean value $\bar{C}_D$ and a superimposed perturbation C_D'. Substitution of the perturbed forms of $\mathbf{V}_e$, $\mathbf{V}$ and C_D into the drag force term in (1) yields, to within first order in perturbation quantities,

$$\mathbf{F}_D=-\tfrac{1}{2}\rho A\bar{C}_D|\bar{w}|\bar{w}\mathbf{k}+\tfrac{1}{2}\rho A\bar{C}_D|\bar{w}|[(u_e'-u')\mathbf{i} +(v_e'-v')\mathbf{j}+2(w_e'-w')\mathbf{k}]-\tfrac{1}{2}\rho AC_D'|\bar{w}|\bar{w}\mathbf{k}. \quad (6)$$

The first term on the right-hand side of (6) is the mean drag force. The second term is the contribution to the drag force from perturbations in the relative wind vector, and the third the contribution from fluctuations in the drag coefficient.

c. The perturbation equations

Utilization of the above concepts and the principle that terms of like order balance yields the first-order perturbation equations that govern the balloon

Unauthenticated | Downloaded 09/20/24 07:16 PM UTC

motion:

$$m\frac{du'}{dt}=\tfrac{1}{2}\rho A\bar{C}_D|\bar{w}|(u_e'-u')+\tfrac{1}{2}\rho AC_{Lx}\bar{w}^2+m_a\frac{d}{dt}(u_e'-u'), \quad (7)$$

$$m\frac{dv'}{dt}=\tfrac{1}{2}\rho A\bar{C}_D|\bar{w}|(v_e'-v')+\tfrac{1}{2}\rho AC_{Ly}\bar{w}^2+m_a\frac{d}{dt}(v_e'-v'), \quad (8)$$

$$m\frac{dw'}{dt}=\rho A\bar{C}_D|\bar{w}|(w_e'-w')-\tfrac{1}{2}\rho A\bar{w}|\bar{w}|C_D'+m_a\frac{d}{dt}(w_e'-w'). \quad (9)$$

The zero-order or unperturbed state is given by

$$\tfrac{1}{2}\rho A\bar{C}_D|\bar{w}|\bar{w}=(m_0-m)g. \quad (10)$$

In deriving (7)–(9), it was assumed that the environmental wind field has negligible horizontal and temporal variations, i.e., $\mathbf{V}_e'$ is a function of altitude z only, so that the time derivatives of the environmental wind components in (7)–(9) are the changes in the environmental wind as would be seen by an observer attached to the balloon [see Fichtl (1971) for more details]. The first-order equations will be used in the analysis that follows. In these equations, the lift forces are confined to the horizontal plane, and the fluctuating portion of the drag force resulting from fluctuations in the drag coefficient is confined to the vertical.

4. Fourier-Stieltjes representation and rms aerodynamic coefficients

The time-dependent quantities in (7)–(9) can be represented with Fourier-Stieltjes integrals, i.e.,

$$\xi(t)=\int_{-\infty}^{\infty}e^{i\omega t}dZ_\xi(\omega), \quad (11)$$

where $\xi(t)$ is a time-dependent quantity, and $dZ_\xi(\omega)$ the complex Fourier amplitude of $\xi(t)$ at frequency ω.

The equations that govern the Fourier amplitudes of the time-dependent quantities in (7)–(9) are obtained by substituting their Fourier-Stieltjes representations into these equations and noting that the functions $\exp(i\omega t)$ constitute a complete orthogonal function set, so that

$$dZ_u(\omega)=\left(\frac{1+i\mu\omega T}{1+i\omega T}\right)dZ_{u_e}(\omega)+\frac{|\bar{w}|}{\bar{C}_D}\left(\frac{dZ_x(\omega)}{1+i\omega T}\right), \quad (12)$$

$$dZ_v(\omega)=\left(\frac{1+i\mu\omega T}{1+i\omega T}\right)dZ_{v_e}(\omega)+\frac{|\bar{w}|}{\bar{C}_D}\left(\frac{dZ_y(\omega)}{1+i\omega T}\right), \quad (13)$$

$$dZ_w(\omega)=\left(\frac{2+i\mu\omega T}{2+i\omega T}\right)dZ_{w_e}(\omega)-\frac{\bar{w}}{\bar{C}_D}\left(\frac{dZ_z(\omega)}{2+i\omega T}\right), \quad (14)$$

where $dZ_{x,y,z}$ are the Fourier amplitudes of $C_{Lx,y}$ and C_D', and the quantities T and μ are given by

$$T=\frac{m+m_a}{|m_0-m|}\frac{|\bar{w}|}{g}, \quad (15)$$

$$\mu=\frac{m_a}{m+m_a}. \quad (16)$$

The first terms on the right-hand sides of (12)–(14) are the contributions to the balloon Fourier amplitudes resulting from environmental forcing (Fichtl, 1971). The second terms are the contributions arising from fluctuations in the aerodynamic coefficients. We shall assume that the Fourier amplitudes of the environmental wind are uncorrelated with the corresponding Fourier amplitudes of the aerodynamic coefficients, so that the fluctuating aerodynamic terms in (12)–(14) can be analyzed separately. This useful hypothesis is commonly invoked in the engineering community in problems of a similar nature (Wood and Berry, 1962). The fluctuating aerodynamic terms in (12)–(14) can be expressed as

$$\left.\begin{aligned}dZ_1&=\frac{|\bar{w}|}{\bar{C}_D}\exp(i\chi_1)\frac{dZ_x(\omega)}{[1+(\omega T)^2]^{\frac{1}{2}}}\\ dZ_2&=\frac{|\bar{w}|}{\bar{C}_D}\exp(i\chi_1)\frac{dZ_y(\omega)}{[1+(\omega T)^2]^{\frac{1}{2}}}\\ dZ_3&=\frac{|\bar{w}|}{\bar{C}_D}\exp(i\chi_2)\frac{dZ_z(\omega)}{[4+(\omega T)^2]^{\frac{1}{2}}}\end{aligned}\right\}, \quad (17)$$

where

$$\left.\begin{aligned}\chi_1&=\tan^{-1}(-\omega T)\\ \chi_2&=\frac{\pi}{2}\left(1+\frac{\bar{w}}{|\bar{w}|}\right)+\tan^{-1}\left(-\frac{\omega T}{2}\right)\end{aligned}\right\}. \quad (18)$$

The quantity χ_1 is the phase angle of the zonal and meridional components of the induced lift force relative to the corresponding components of induced velocity, and χ_2 the phase angle of the vertical component of the induced fluctuating drag force relative to the induced vertical velocity. These results imply that the induced aerodynamic lift force leads the corresponding induced horizontal component of velocity. For a rising balloon ($\bar{w}>0$), the induced vertical drag force lags the induced vertical velocity, and vice versa for the falling balloon ($\bar{w}<0$). Fig. 1 shows χ_1 and χ_2 as functions of ωT for the rising balloon case. The phase angles for the falling balloon can be obtained from Fig. 1 by subtracting π radians from χ_2.

Unauthenticated | Downloaded 09/20/24 07:16 PM UTC

The relationship between the spectra of the aerodynamic coefficients, $\phi_{x,y,z}(\omega)$, and the associated aerodynamically induced balloon motion, $\psi_{u,v,w,}(\omega)$, can be obtained by multiplying each of (17) by its complex conjugate and performing an ensemble average over all realizations, to yield

$$\phi_x(\omega)=\frac{\bar{C}_D{}^2}{\bar{w}^2}[1+(\omega T)^2]\psi_u(\omega), \tag{19}$$

$$\phi_y(\omega)=\frac{\bar{C}_D{}^2}{\bar{w}^2}[1+(\omega T)^2]\psi_v(\omega), \tag{20}$$

$$\phi_z(\omega)=\frac{\bar{C}_D{}^2}{\bar{w}^2}[4+(\omega T)^2]\psi_w(\omega). \tag{21}$$

Eqs. (19) and (20) are of the same form, so that for mathematical purposes only one need be considered.

The rms lift and drag coefficients can be obtained by integrating (19) and (21) over the domain $-\infty<\omega<\infty$ with the result

$$C^2{}_{L\text{rms}}=\bar{C}_D{}^2\frac{\sigma_u{}^2}{\bar{w}^2}\int_0^\infty[1+(\omega T)^2]\Phi_u(\omega)d\omega, \tag{22}$$

$$C^2{}_{D\text{rms}}=\bar{C}_D{}^2\frac{\sigma_w{}^2}{\bar{w}^2}\int_0^\infty[4+(\omega T)^2]\Phi_w(\omega)d\omega, \tag{23}$$

where σ_u and σ_w are the standard deviations of the zonal and vertical self induced velocity components, and $\Phi_u(\omega)$ and $\Phi_w(\omega)$ are the corresponding normalized spectra referenced to the half-interval $0<\omega<\infty$, i.e., $\Phi_u(\omega)=2\sigma_u{}^{-2}\psi_u(\omega)$ and $\Phi_w(\omega)=2\sigma_w{}^{-2}\psi_w(\omega)$. These equations facilitate the calculation of the rms aerodynamic coefficients from relatively simple measurements of aerodynamically induced sensor motions, and are general in the sense that they apply to narrow and broad band aerodynamic processes.

5. Aerodynamic coefficients for narrow band aerodynamic processes

If the aerodynamic processes are sufficiently narrow in frequency content, the calculation of the rms aerodynamic coefficients with Eqs. (22) and (23) becomes relatively simple. A useful representation of a narrow band process is

$$\Phi(\omega)=\left[\frac{1}{1-F(-\omega_0/\epsilon)}\right]\times\frac{\exp[-(\omega-\omega_0)^2/2\epsilon^2]}{\epsilon(2\pi)^{\frac{1}{2}}},\quad 0<\omega<\infty, \tag{24}$$

where

$$F(-\omega_0/\epsilon)=1-\int_{-\omega_0/\epsilon}^{\infty}\frac{1}{(2\pi)^{\frac{1}{2}}}\exp(-\zeta^2/2)d\zeta, \tag{25}$$

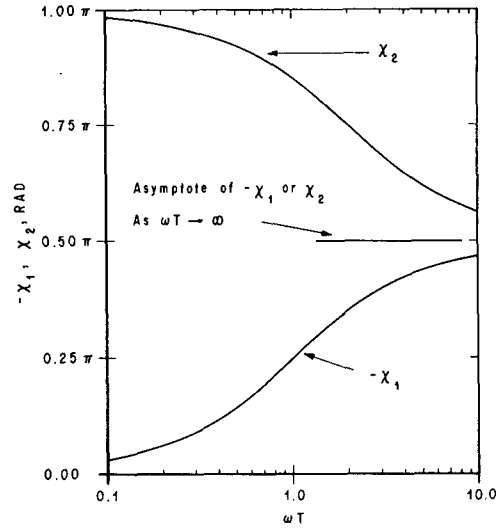

FIG. 1. The phase angles χ_1 and χ_2 of the Fourier components of the first-order aerodynamically induced horizontal lift and vertical drag forces as functions of ωT for the rising balloon ($\bar{w}>0$). For the falling balloon ($\bar{w}<0$), π radians must be subtracted from χ_2.

and ϵ is the measure of the width of the spectrum. The maximum value of $\Phi(\omega)$ occurs at $\omega=\omega_0$. If $\epsilon\to 0$, then

$$\Phi(\omega)\to\delta(\omega-\omega_0), \tag{26}$$

where $\delta(\omega-\omega_0)$ is the Dirac delta function (Lighthill, 1958).

Substitution of (24) into (22) or (23) yields the rms coefficients, namely

$$C_{\text{rms}}{}^2=\bar{C}_D{}^2\frac{\sigma^2}{\bar{w}^2}\left\{[\gamma+T^2(\omega_0{}^2+\epsilon^2)]+\frac{T^2[2\epsilon\omega_0 f(-\omega_0/\epsilon)-\epsilon^2 f'(-\omega_0/\epsilon)]}{1-F(-\omega_0/\epsilon)}\right\}, \tag{27}$$

where $\gamma=1$ for $C_{L\text{rms}}$ and $\gamma=4$ for $C_{D\text{rms}}$, σ is σ_u or σ_w as the case may be,

$$f(\zeta)=\frac{1}{(2\pi)^{\frac{1}{2}}}\exp(-\zeta^2/2), \tag{28}$$

and $f'(-\omega_0/\epsilon)$ denotes the derivative of $f(\zeta)$ with respect to ζ evaluated at $\zeta=-\omega_0/\epsilon$. If the widths of the balloon motion spectra are sufficiently narrow, such that $\omega_0/\epsilon\gtrsim 3$ say, the quantities $f(-\omega_0/\epsilon)$ and $f'(-\omega_0/\epsilon)$ approach zero, so that the second term on the right-hand side of (27) can be neglected, yielding

$$C^2{}_{\text{rms}}=\bar{C}_D{}^2\frac{\sigma^2}{\bar{w}^2}[\gamma+T^2(\omega_0{}^2+\epsilon^2)]. \tag{29}$$

Furthermore, if the balloon motion spectrum is suffi-

Unauthenticated | Downloaded 09/20/24 07:16 PM UTC

ciently narrow that $\epsilon \ll \omega_0$, then

$$C^2_{\text{rms}} = \bar{C}_D{}^2 \frac{\sigma^2}{\bar{w}^2} [\gamma + (\omega_0 T)^2]. \quad (30)$$

This corresponds to the case in which $\Phi(\omega)$ is a Dirac delta function as given by (26).

6. Jimsphere aerodynamic coefficients (roughened balloon)

The experimental data used in this study consist of FPS-16 radar measurements of the Jimsphere balloon. The Jimsphere is a rigid, roughened, 2 m diameter Mylar sphere which is widely used in the aerospace and meteorological communities to obtain accurate, high-resolution measurements of the wind profile in the lowest 18 km of the atmosphere. An internal overpressure of about 5 mb is maintained to ensure constant volume. The balloon has 398 conical roughness elements, each approximately 7.5 cm wide at the base and 7.5 cm high, which serve to control vortex shedding in the supercritical Reynolds number region below 11 km.

The induced motions of rough spherical balloons like the Jimsphere constitute a high-frequency, narrow-band process. To determine the rms lift coefficient of the Jimsphere wind sensor, three Jimsphere ascents, each tracked by two FPS-16 radars, were selected for analysis. The measurements were made between 1300 and 1500 (all times GMT) on 23 December 1964, 18 December 1967, and 19 March 1968, at the Kennedy Space Center, Fla. These tests will be referred to as flights 1, 2 and 3, respectively. The measurements extended over the altitude interval 0.5–16 km. The radar provided range, and elevation and azimuth angle measurements of the balloon's position at 0.1-sec intervals. These data were converted to Cartesian coordinates and corrected for the curvature of the earth. The Cartesian coordinates were differenced over 0.2-sec intervals to yield estimates of the zonal, meridional and vertical velocities of the balloon at 0.1-sec intervals. Spectra of the resulting velocity time histories were used to calculate the rms coefficients of the Jimsphere balloon.

Fig. 2 contains spectra of the zonal, meridional and vertical components of velocity of a Jimsphere for the altitude interval $4.4 < z < 5.4$ km, calculated from FPS-16 radar data taken between 1400 and 1500 on 23 December 1964. The zonal and meridional spectra have peaks at approximately 0.21 Hz. These peaks are attributed to motions which result from the fluctuating aerodynamic lift force. The absence of a pronounced spectral peak in the vertical velocity spectrum at, or close to, 0.21 Hz indicates that the vertical component of induced motion is insignificant and implies that $C_{D\text{rms}} \ll C_{L\text{rms}}$.

If the spectral peaks in Fig. 2 are associated with a spiral motion as observed by Scoggins (1967), then the

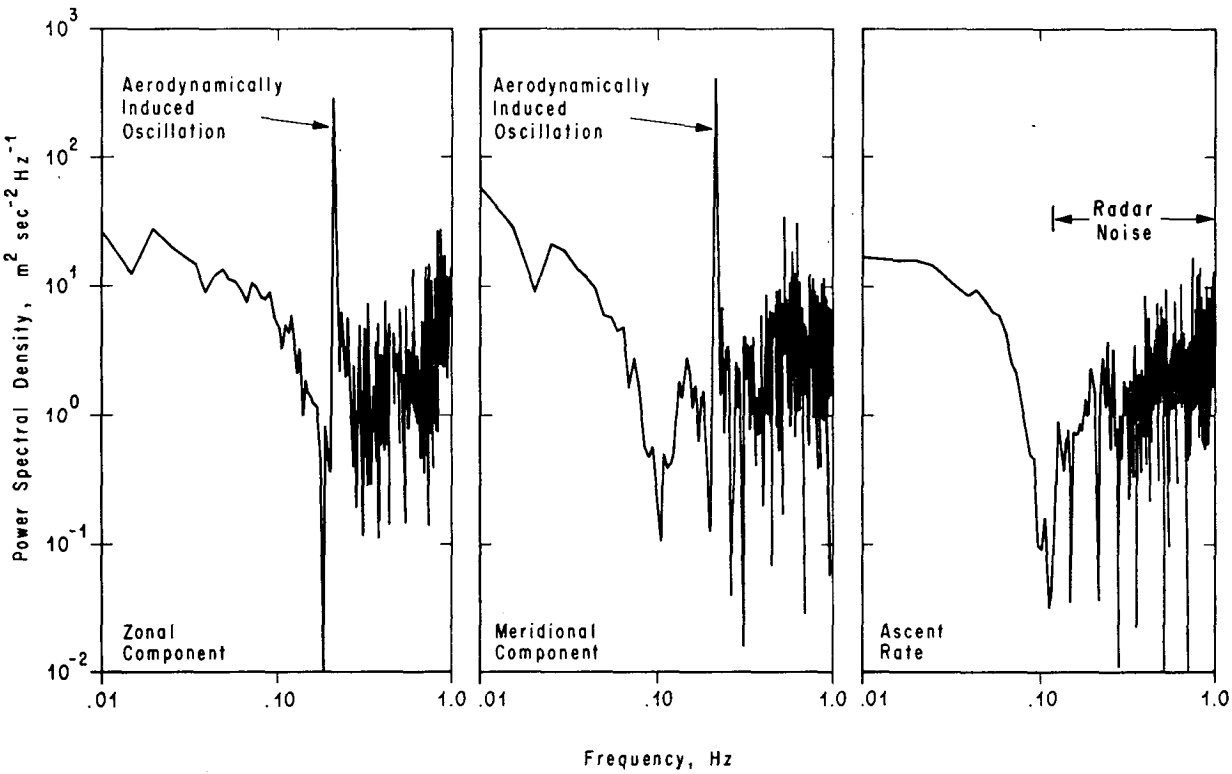

FIG. 2. Power spectra of the zonal, meridional and vertical components of velocity of a Jimsphere balloon for the height interval $4.4 < z < 5.4$ km.

Unauthenticated | Downloaded 09/20/24 07:16 PM UTC

zonal and meridional components should be out of phase by 90°. To verify this observation, Jimsphere velocity component data, sampled at 0.1-sec intervals, were filtered with a Martin-Graham (Graham, 1963) narrow band-pass filter, the response function of which is shown in Fig. 3. The samples of filtered data shown in Fig. 4 clearly exhibit the expected phase relationship. Fig. 4 also suggests that the vertical component of induced motion, if it exists, is very small.

As a constant diameter spherical wind sensor ascends through the atmosphere, the Reynolds number

$$\mathrm{Re}=\frac{|\bar{w}|D}{\nu} \tag{31}$$

decreases because the coefficient of kinematic viscosity ν usually increases with height while the rise rate $|\bar{w}|$ usually decreases slowly. The quantity D is the diameter of the sensor. Since the aerodynamic properties of spheres depend on the Reynolds number, one should expect a dependence of the lift coefficient on altitude. Accordingly, the balloon velocity time histories were divided into 1-km altitude segments to calculate the rms lift coefficients of the Jimsphere.

Spectra of the zonal, meridional and vertical components of balloon velocity were calculated for each time-history segment using the fast-Fourier transform method. This yielded 15 spectra for each component of velocity for each of the six radar tracks, or a total of 270 spectra. Since the typical rise rate of the Jimsphere is about 5 m sec^{-1}, each spectrum was based on a time-history segment containing ~2000 data points. The vertical velocity spectrum shown in Fig. 2 was typical in that it did not reveal any obvious vertical component of aerodynamically induced motion. It was assumed that the spectra of the zonal and meridional components of induced velocity are of the form given by (24). A careful

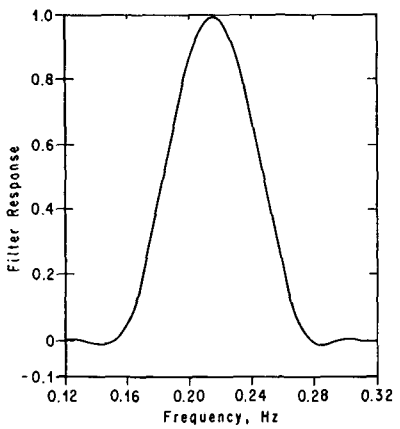

FIG. 3. The response function of the band-pass filter used to isolate the aerodynamically induced portion of the Jimsphere's motion.

examination of the spectra showed this representation to be reasonable. In the case of the Jimsphere balloon, $F(-\omega_0/\epsilon)$ is approximately 0; thus, the nondimensional spectrum is given by

$$\omega_0\Phi_u(\omega)=\frac{1}{(2\pi)^{\frac{1}{2}}\alpha}\exp[-(1-\omega/\omega_0)^2/2\alpha^2], \tag{32}$$

where $\alpha=\epsilon/\omega_0$ is assumed to be a universal constant. The parameters ω_0 and σ_u define the spectrum $\Phi_u(\omega)$ and it is assumed that these quantities, rendered in nondimensional form by division by $|\bar{w}|/D$ and $|\bar{w}|$, are universal functions of the Reynolds number, so that

$$\left.\begin{aligned}\frac{\omega_0 D}{|\bar{w}|}&=\mathrm{S}=F_1(\mathrm{Re})\\ \left(\frac{\sigma_u}{\bar{w}}\right)^2&=F_2(\mathrm{Re})\end{aligned}\right\}. \tag{33}$$

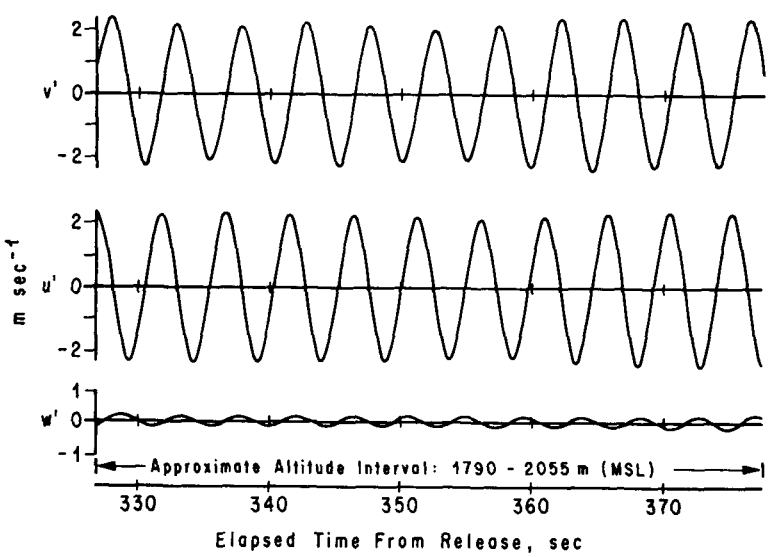

FIG. 4. Example of balloon velocity component measurements which were filtered to isolate the aerodynamically induced motions of the Jimsphere.

Unauthenticated | Downloaded 09/20/24 07:16 PM UTC

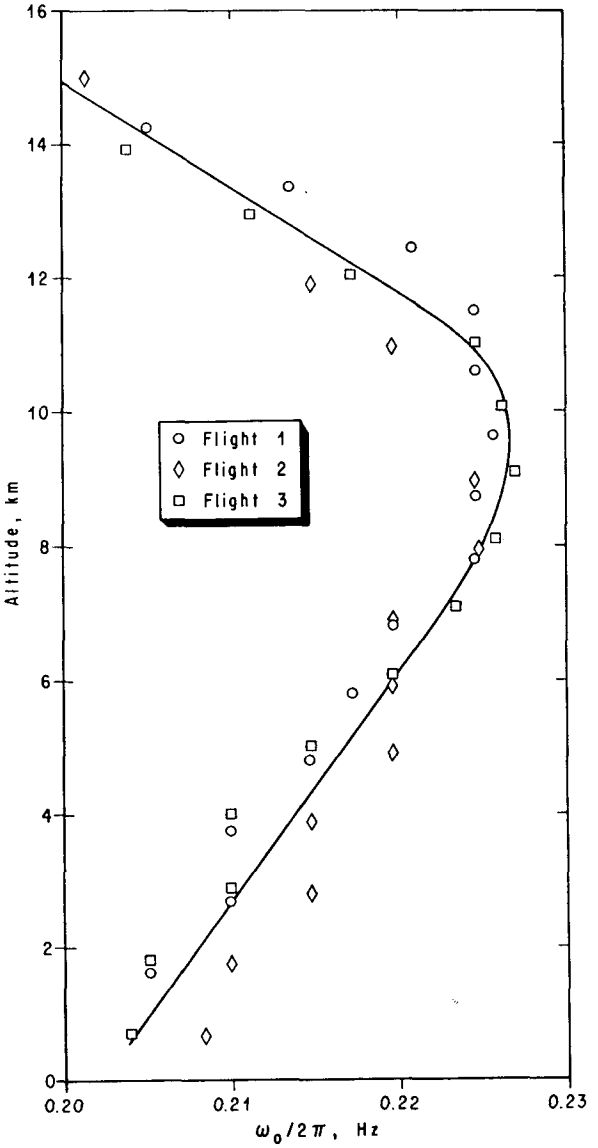

FIG. 5. The frequency $\omega_0/(2\pi)$ at the spectral peak associated with the aerodynamically induced motion of the Jimsphere as a function of altitude.

The nondimensional frequency S is called the Strouhal number. In aerodynamic parlance the Strouhal number usually refers to the nondimensional frequency of the dominant Fourier component in the wake. Here, it is used to denote the nondimensional frequency of the sensor. It is not quite necessarily true *a priori* that the frequency of the wake is equal to that of the induced motion of the body. The numerical value of α was obtained experimentally by determining that value of ω/ω_0, ω^*/ω_0, say, at which $\omega_0\Phi_u(\omega)$ is equal to one-tenth of the peak value; that is, $\omega_0\Phi_u(\omega^*)=0.1\omega_0\Phi_u(\omega_0)=0.1[(2\pi)^{\frac{1}{2}}\alpha]^{-1}$. Substitution of ω^*/ω_0 into (32) yields

$$\alpha=\frac{1-\omega^*/\omega_0}{(2\ln 10)^{\frac{1}{2}}}. \tag{34}$$

This expression was used to compute α for each horizontal velocity spectrum. The various values of α showed no dependence on height or Reynolds number and the expected value of α was found to be 0.00906.

The frequency ω_0 of the peak of the aerodynamically induced spectrum and the area σ_u^2 under the spectrum were used to calculate the nondimensional functions $F_1(\mathrm{Re})$ and $F_2(\mathrm{Re})$. Figs. 5 and 6 show $\omega_0/2\pi$ and σ_u^2 as functions of altitude. Each of the plotted points represents a 1-km segment of one balloon flight, and was obtained by averaging values from four spectral estimates. The four spectra represent the zonal and meridional components derived from each of the two radars. A smooth line was drawn through each set of plotted data. The smoothed values of $\omega_0/2\pi$ and σ_u^2, the standard profile of $\bar{w}$ as a function of altitude calculated by DeMandel and Krivo (1971), and the standard profile of ν (*U. S. Standard Atmosphere Supplements,*

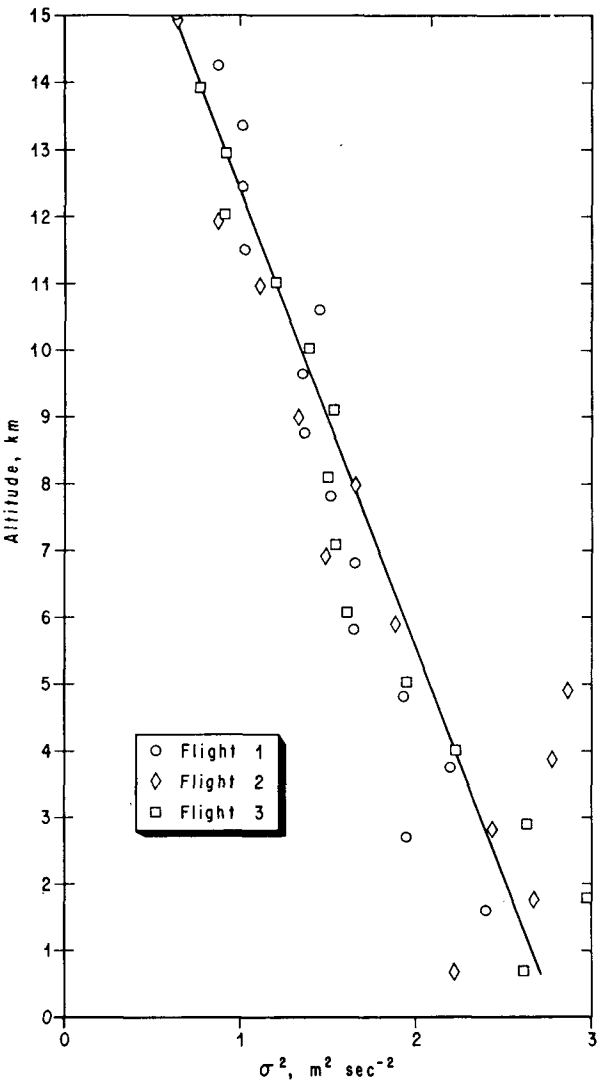

FIG. 6. The variance σ_u^2 of the aerodynamically induced motion of the Jimsphere as a function of altitude.

Unauthenticated | Downloaded 09/20/24 07:16 PM UTC

1966) were used to calculate the nondimensional functions $F_1(\mathrm{Re})$ and $F_2(\mathrm{Re})$. These functions correspond to the Strouhal number and the nondimensional zonal or meridional velocity variance $(\sigma_u/\bar{w})^2$ (Figs. 7 and 8). Fig. 7 shows that the Strouhal number has a typical value of 0.55 and a maximum of nearly 0.60 at $\mathrm{Re}=2.5\times10^5$. It is noteworthy that the Strouhal number attains a maximum in the neighborhood of $\mathrm{Re}=2.5\times10^5$ which is the Reynolds number associated with transition of smooth balloons from subcritical to supercritical conditions (Wright, 1967). It is tempting to speculate that a type of transition is also present in the neighborhood of $\mathrm{Re}=2.5\times10^5$ for rough spheres like the Jimsphere. Fig. 8 shows that the nondimensional variance is a monotonically increasing function of the Reynolds number in the interval $1.4\times10^5<\mathrm{Re}<6.7\times10^5$, with values ranging between 0.03 and 0.092.

The final parameters needed to calculate the rms lift coefficient are the nondimensional time constant

$$\tau=\frac{T|\bar{w}|}{D}, \tag{35}$$

and the mean drag coefficient $\bar{C}_D$ of the Jimsphere. Fichtl (1971) calculated the time constant T as a function of altitude for the Jimsphere. Substitution of T and $\bar{w}$ into (35) and plotting the resulting values of τ as a function of Reynolds number yields the curve in Fig. 9. Fig. 10 contains a plot of $\bar{C}_D$ as a function of Reynolds number.

In view of the fact that α is extremely small with respect to unity, the spectra of the zonal and meridional velocity components of the Jimsphere's aerodynamically induced motion may be treated as Dirac delta functions. This means that (30) is applicable to the problem.

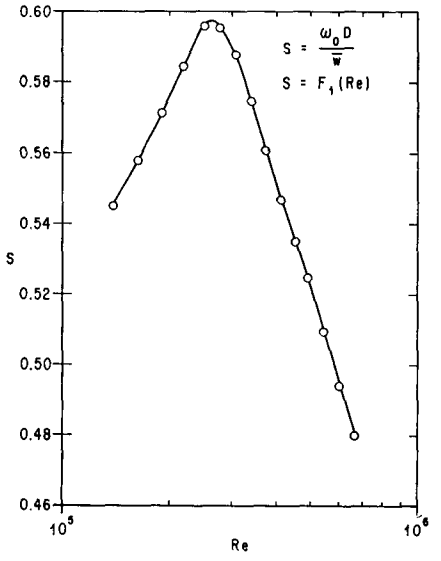

FIG. 7. The Strouhal number S of the Jimsphere balloon as a function of Reynolds number.

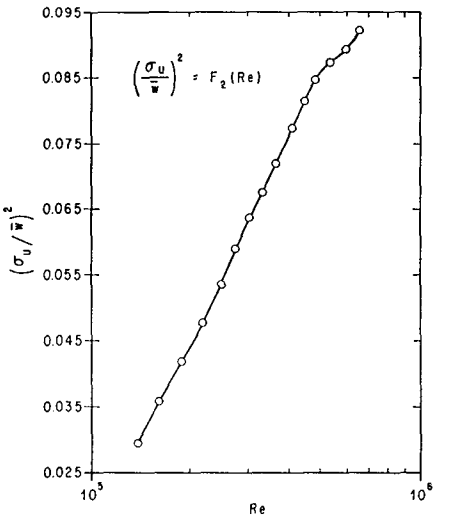

FIG. 8. The nondimensional zonal or meridional velocity variance $(\sigma_u/\bar{w})^2$ as a function of Reynolds number.

The equation for the lift coefficient can be written in terms of S and τ as

$$C^2_{L\mathrm{rms}}=\bar{C}_D{}^2\frac{\sigma_u{}^2}{\bar{w}^2}[1+(S\tau)^2]. \tag{36}$$

Substitution of S, $(\sigma_u/\bar{w})^2$, τ and $\bar{C}_D$, as given in Figs. 7–10, into (36) yields the rms lift coefficient as a function of Reynolds number (Fig. 10). Fig. 10 shows that the $C_{L\mathrm{rms}}$ and $\bar{C}_D$ curves have similar shapes and a typical ratio $C_{L\mathrm{rms}}/\bar{C}_D$ of 0.36. The transition-like phenomenon previously mentioned with regard to S appears to be evident in the steady-state drag and rms lift coefficient curves in the neighborhood of $\mathrm{Re}=2.5\times10^5$.

The phase angles of the time-dependent aerodynamic lift and drag coefficients for the Jimsphere at frequency

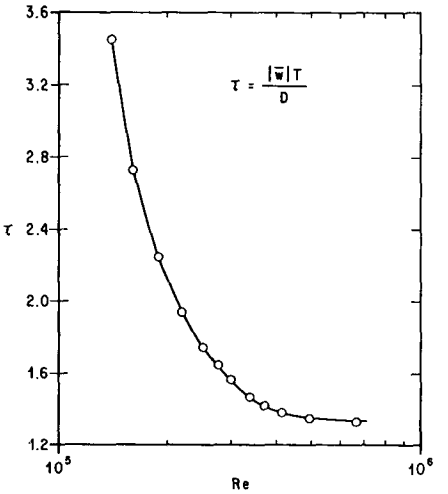

FIG. 9. The nondimensional time constant τ of the Jimsphere as a function of Reynolds number.

Unauthenticated | Downloaded 09/20/24 07:16 PM UTC

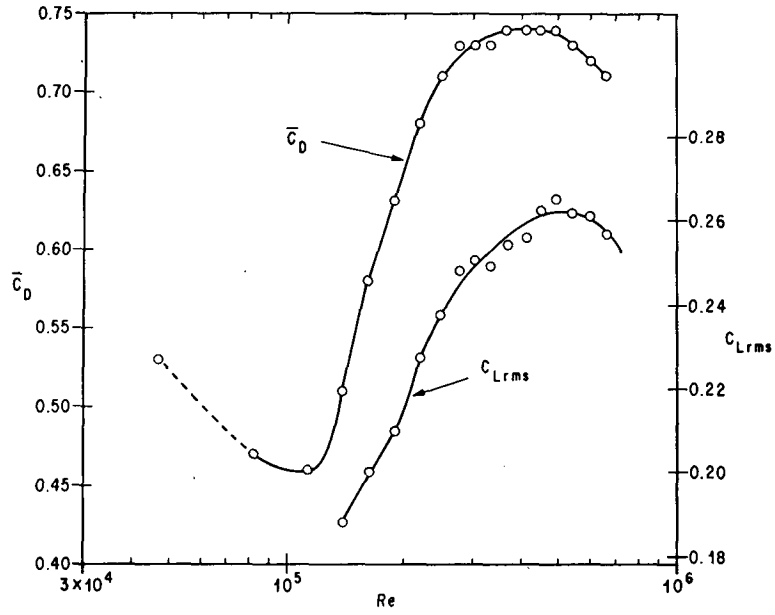

FIG. 10. The mean drag coefficient $\bar{C}_D$ and the rms lift coefficient C_{Lrms} as functions of Reynolds number.

ω_0 are given by

$$\left.\begin{aligned}\chi_1&=\tan^{-1}(-S\tau)\\ \chi_2&=\pi+\tan^{-1}\left(-\frac{S\tau}{2}\right)\end{aligned}\right\}. \tag{37}$$

Since S and τ are functions of the Reynolds number, so also are χ_1 and χ_2. Fig. 11 gives χ_1 and χ_2 as functions of Re based on the data in Figs. 7 and 9. The phase angle χ_1 is equal to the angle between the aerodynamically induced lift vector and the induced velocity vector of the balloon in the horizontal plane. In the horizontal, the balloon executes simple harmonic circular motion and the component of horizontal tangential lift in the direction of the induced motion balances the horizontal component of drag, associated with $\bar{C}_D$, which results from the horizontal induced motion of balloon. In addition, there is a horizontal component of induced aerodynamic lift perpendicular to the circular horizontal path of the balloon which is directed inward and provides the necessary force needed to balance the apparent forces which result from the horizontal induced centripetal acceleration of the balloon. Since $\chi_2 \neq 0$ or π radians, the induced drag, if it exists, associated with C_D' in the vertical alternately enhances and degrades in time the vertical drag associated with $\bar{C}_D$ and the induced vertical velocity [see Eq. (9)].

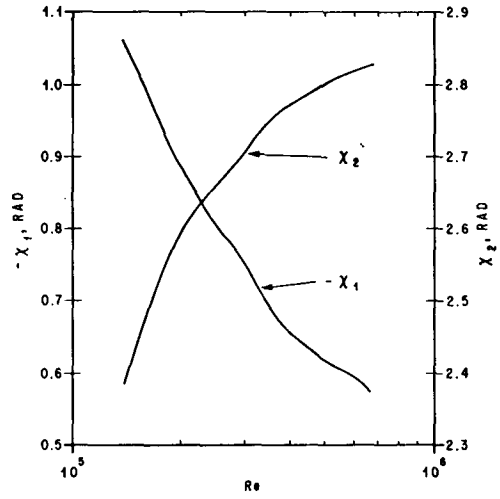

FIG. 11. The phase angles $\chi_1(S\tau)$ and $\chi_2(S\tau)$ of the Fourier components associated with the first-order aerodynamically induced horizontal lift and vertical drag forces as functions of Reynolds number for the Jimsphere.

7. ROSE aerodynamic lift coefficient (smooth balloon)

As a second example of the application of the theory the 2 m ROSE balloon operating at supercritical Reynolds numbers ($Re > 2.5\times10^5$) is considered. The ROSE is a smooth, aluminized, superpressure sphere which rises at a rate of $\sim$7 m sec^{-1}. This balloon experiences erratic horizontal motions resulting from aerodynamic lift forces.

Rogers and Camnitz (1965) analyzed high-qualtiy Doppler radar tracking data of the ROSE below 7 km and found that the nondimensional spectrum of the aerodynamically induced velocity fluctuations at supercritical Reynolds numbers is well represented by

$$\omega_0\Phi(\omega)=\frac{1}{0.2(2\pi)^{\frac{1}{2}}}\exp\left[\frac{-(1-\omega/\omega_0)^2}{0.08}\right], \tag{38}$$

Unauthenticated | Downloaded 09/20/24 07:16 PM UTC

which implies $\alpha=0.2$. Thus, the nondimensional spectral bandwidth of this process is approximately twenty times greater than that of the Jimsphere. The parameters which define this spectrum are $\sigma_u=2.6$ m sec^{-1} and $\omega_0=0.94$ rad sec^{-1}. The time constant $T\approx 0.64$ sec for the 2 m ROSE in the altitude range under consideration. In the supercritical Reynolds number region Rogers and Camnitz found that $\bar{C}_D\approx 0.3$. Substitution of (38) and the above-mentioned parameters into (22) yields $C_{L\text{rms}}\approx 0.13$. This result should be contrasted with that of Willmarth and Enlow (1969) who find that $C_{L\text{rms}}\approx 0.06$ based on wind tunnel tests of fixed smooth spheres in supercritical Reynolds number flow. This difference cannot be attributed to experimental error and can only be explained by the fact that in one case the balloon is free to respond to the imposed aerodynamic forces. This result should caution investigators to exercise judgement when applying wind tunnel data for constrained bodies to bodies like balloons, falling spheres, etc., which are free to respond to the aerodynamic forces.

8. Summary and conclusions

The aerodynamic properties of rough spherical wind sensors are derived using linear perturbation expansions of the equations of sensor motion and FPS-16 radar measurements of the Jimsphere balloon. Integral relationships between the first-order rms drag and horizontal lift coefficients are obtained from the first-order perturbation equations. These relationships permit the computation of the rms lift and drag coefficients from measurements of the mean drag coefficient, the mean vertical velocity, the time constant of the sensor, and spectral estimates of the velocity components of the aerodynamically induced balloon motion. Although these relationships reduce to rather simple equations for the narrow band processes of rough balloons, the mathematical analysis also can be applied to the more broad band motions of smooth sensors.

Velocity spectra of radar measurements of the Jimsphere show that the aerodynamically induced motions are extremely narrow banded; they behave essentially as a sinusoidal function. The observed aerodynamically induced motions are predominantly horizontal, and it is concluded that the first-order rms drag coefficient is very small compared to the horizontal rms lift coefficient. These results agree with the earlier findings of Scoggins (1967). The horizontal rms lift coefficient is approximately equal to $0.36\bar{C}_D$. The nondimensional induced zonal or meridional velocity variance, Strouhal number, and the horizontal rms lift coefficient are shown to be functions of the Reynolds number. They are also thought to be functions of the mass ratio m/m_0. It would be difficult to determine how the Strouhal number and nondimensional velocity variance depend on m/m_0, however, because many sensor configurations would be required to cover a sufficiently wide range of m/m_0.

The mechanism which produces the aerodynamic motion of rough or smooth balloons is rather complicated. It is obvious that the periodic x- and y-directed aerodynamic lift forces result from the shedding of vorticity and the associated unstable wake of the balloon. However, a detailed investigation of the flow field in the vicinity of the balloon would be needed to reveal the precise nature of the instability which produces the oscillating wake.

REFERENCES

Brockman, W. E., 1964: Small scale wind shears from ROSE balloon tracked by AN/FPS-16 radar. Final Rept., AF 19(604)-7450, University of Dayton, 85 pp.

DeMandel, R. E., and S. J. Krivo, 1971: Radar/balloon measurement of vertical air motions between the surface and 15 km. *J. Appl. Meteor.*, **10**, 313-319.

Engler, N. A., 1965: Development of methods to determine wind, density, pressure, and temperature from the Robin falling balloon. Final Rept., AF 19(604)-7450, University of Dayton, 141 pp.

Fichtl, G. H., 1971: The responses of balloon and falling sphere wind sensors in turbulent flows. NASA TN D-7049, Marshall Space Flight Center, Huntsville, Ala., 26 pp.

Graham, Ronald J., 1963: Determination and analysis of numerical smoothing weights. NASA Tech. Rept. R-179, Marshall Space Flight Center, Huntsville, Ala., 28 pp.

Lighthill, M. J., 1958: *Introduction to Fourier Analysis and Generalized Functions.* New York, Cambridge University Press, 79 pp.

Reed, Wilmer H., III, 1963: Dynamic response of rising and falling balloon wind sensors with application to estimates of wind loads on launch vehicles. NASA Tech. Note D-1821, 31 pp.

Rogers, R. R., and H. G. Camnitz, 1965: Project Baldy, an investigation of aerodynamically-induced balloon motions. Final Rept., NAS8-11140, Cornell Aeronautical Laboratory, Inc., 80 pp.

Scoggins, J. R., 1967: Sphere behavior and the measurement of wind profiles. NASA Tech. Note D-3994, Marshall Space Flight Center, Huntsville, Ala., 53 pp.

U. S. Standard Atmosphere Supplements, 1966: Environmental Science Services Administration, National Aeronautics and Space Administration, and U. S. Air Force, Government Printing Office, Washington, D. C., 289 pp.

Willmarth, W. W., and R. L. Enlow, 1969: Aerodynamic lift and moment fluctuations of a sphere. *J. Fluid Mech.*, **36**, 417-432.

Wood, J. D., and J. G. Berry, 1962: Random excitation of missiles due to winds. *Proceedings of the National Symposium on Winds for Aerospace Vehicle Design*, Vol. 1, AFCRL-62-273(I), Surveys in Geophysics No. 140, Vol. 1, 125-138.

Wright, John B., 1967: Reynolds number effects on ascending spherical balloons. *J. Space. Rockets*, **4**, 407-408.

Unauthenticated | Downloaded 09/20/24 07:16 PM UTC